The Astrophysical Journal, 908:140 (9pp), 2021 February 20 https://doi.org/10.3847/1538-4357/abd9b9

Spins of Primordial Black Holes Formed in the Radiation-dominated Phase of the Universe: First-order Effect

Tomohiro Harada[1], Chul-Moon Yoo[2], Kazunori Kohri[3,4,5], Yasutaka Koga[1], and Takeru Monobe[1]
[1] Department of Physics, Rikkyo University, Toshima, Tokyo 171-8501, Japan; harada@rikkyo.ac.jp
[2] Gravity and Particle Cosmology Group, Division of Particle and Astrophysical Science, Graduate School of Science, Nagoya University, Nagoya 464-8602, Japan
[3] Institute of Particle and Nuclear Studies, KEK, 1-1 Oho, Tsukuba, Ibaraki 305-0801, Japan
[4] The Graduate University for Advanced Studies (SOKENDAI), 1-1 Oho, Tsukuba, Ibaraki 305-0801, Japan
[5] Kavli Institute for the Physics and Mathematics of the Universe (WPI), University of Tokyo, Kashiwa 277-8583, Japan
Received 2020 October 30; revised 2020 December 23; accepted 2021 January 5; published 2021 February 19

Abstract

The standard deviation of the initial values of the nondimensional Kerr parameter a_* of primordial black holes (PBHs) that formed in the radiation-dominated phase of the universe is estimated to the first order of perturbation for the narrow power spectrum. Evaluating the angular momentum at turnaround based on linearly extrapolated transfer functions and peak theory, we obtain the expression $\sqrt{\langle a_*^2\rangle} \simeq 4.0\times10^{-3}(M/M_H)^{-1/3}\sqrt{1-\gamma^2}[1-0.072\log_{10}(\beta_0(M_H)/(1.3\times10^{-15}))]^{-1}$, where M_H, $\beta_0(M_H)$, and γ are the mass within the Hubble horizon at the horizon entry of the overdense region, the fraction of the universe which collapsed to PBHs at the scale of M_H, and a quantity that characterizes the width of the power spectrum, respectively. This implies that for $M\simeq M_H$, the higher the probability of the PBH formation, the larger the standard deviation of the spins, while PBHs of $M\ll M_H$ that formed through near-critical collapse may have larger spins than those of $M\simeq M_H$. In comparison to the previous estimate, the new estimate has an explicit dependence on the ratio $M/M_{\rm H}$ and no direct dependence on the current dark matter density. On the other hand, it suggests that the first-order effect can be numerically comparable to the second-order one.

Unified Astronomy Thesaurus concepts: Primordial black holes (1292)

1. Introduction

Recently, primordial black holes (PBHs) have been intensively investigated not only as a realistic candidate for dark matter (Carr et al. 2010, 2016, 2017, 2020) but also as a possible origin of black holes of tens of solar masses that are the source of gravitational waves detected by LIGO and Virgo (Nakamura et al. 1997; Bird et al. 2016; Sasaki et al. 2016; Clesse & García-Bellido 2017; Raidal et al. 2017). Various mechanisms generating PBHs have been proposed. Among them, we will focus on PBHs formed as a result of the collapse of the primordial cosmological perturbation. After inflation generates perturbations at super-horizon scales, the scales successively enter the Hubble horizon in the radiation-dominated phase and the perturbations can collapse to form PBHs if the amplitude of the perturbation exceeds some threshold value. The threshold values have been studied in terms of $\bar{\delta}_H$, the density perturbation averaged over the overdense region at horizon entry (Carr 1975; Polnarev & Musco 2007; Musco et al. 2009; Harada et al. 2013, 2015; Musco & Miller 2013), although this is currently discussed in a more sophisticated way based on the compaction function (Shibata & Sasaki 1999; Germani & Musco 2019; Musco 2019; Escrivà 2020; Escrivà et al. 2020) and peak theory (Yoo et al. 2018, 2021). Roughly speaking, the mass of the PBH is given by the mass M_H contained within the Hubble horizon at the time of horizon entry t, where $M_H\sim c^3t/G$, although for the near-critical case $\bar{\delta}_H\simeq\bar{\delta}_{H,\rm th}$, the scaling law $M/M_H\propto(\bar{\delta}_H-\bar{\delta}_{H,\rm th})^\beta$ with $\beta\simeq0.36$ implies the formation of PBHs of $M\ll M_H$ (Niemeyer & Jedamzik 1999; Musco et al. 2009; Musco & Miller 2013).

Thanks to the uniqueness theorem, isolated stationary black holes in vacuum are perfectly characterized by two parameters, the mass M and the spin angular momentum $\boldsymbol{S}$. Alternatively, we can use the nondimensional spin angular momentum $\boldsymbol{a}_*=\boldsymbol{S}c/GM^2$. The statistical distribution of the spins is a key probe into the origin of black holes. In the gravitational-wave observation of binary black holes by LIGO and Virgo, the effective spin parameter $\chi_{\rm eff}$ can be measured. Up to now, the observed data for most binary black holes have been consistent with $\chi_{\rm eff}=0$ (Abbott et al. 2019), although there are some exceptions (Abbott et al. 2020).

PBHs may have changed their spins from their initial values. PBHs have evaporated away through Hawking radiation if their masses are smaller than $\sim10^{15}$ g. The spin of the black hole enhances the Hawking radiation and deforms its spectrum. A spinning black hole decreases its nondimensional Kerr parameter $a_*:=\sqrt{\boldsymbol{a}_*\cdot\boldsymbol{a}_*}$ through the Hawking radiation, while a black hole much more massive than $\sim10^{15}$ g does not significantly change a_* through the Hawking radiation (Page 1976; Arbey et al. 2020; Dasgupta et al. 2020). PBHs change their spins very little in the radiation-dominated phase (Chiba & Yokoyama 2017), while it is proposed that mass accretion could change the spin of black holes in some cosmological scenarios (e.g., De Luca et al. 2020).

In this paper, we investigate the initial values of the spins of PBHs. Recently, this issue has been discussed by many authors from different points of view (Chiba & Yokoyama 2017; Harada et al. 2017; De Luca et al. 2019; He & Suyama 2019; Mirbabayi et al. 2020). Among them, De Luca et al. (2019) apply Heavens & Peacock's (1988) approach to the first-order effect of perturbation and give a clear expression, $\sqrt{\langle a_*^2\rangle}\sim\Omega_{\rm dm}\tilde{\sigma}_H\sqrt{1-\gamma^2}/\pi$, where $\Omega_{\rm dm}$, $\tilde{\sigma}_H$, and $\gamma:=\langle k^2\rangle/\sqrt{\langle k^4\rangle}$ are the current ratio of the dark matter component to the critical density, the standard deviation of the

density perturbation at horizon entry of the inverse wavenumber, and a quantity that characterizes the width of the power spectrum, respectively. In this paper, we apply the same approach to this issue but reach a different result. This paper is organized as follows. In Section 2, we define the angular momentum and give its expression to the first order of perturbation in the region that collapses to a PBH. In Section 3, we estimate the angular momentum at the turnaround under the assumption of a narrow spectrum. In Section 4, we estimate the nondimensional Kerr parameter of the PBH. Section 5 is devoted to the summary and a discussion, in particular in comparison to previous works. We use units in which $c = 1$ in this paper.

2. Angular Momentum

2.1. Definition

We follow De Luca et al. (2019) for the definition of angular momentum. If the spacetime admits a Killing vector field ϕ_i^a, which is tangent to a spacelike hypersurface and generates a spatial rotation on it, the angular momentum $S_i(\Sigma)$ contained in the region Σ on the spacelike hypersurface can be defined as a conserved charge in terms of the integral on the boundary $\partial\Sigma$ as (Wald 1984)

$$S_i(\Sigma) := \frac{1}{16\pi G}\int_{\partial\Sigma}\epsilon_{abcd}\nabla^c(\phi_i)^d = -\frac{1}{8\pi G}\int_{\Sigma}R^{ab}n_a(\phi_i)_b d\Sigma \tag{1}$$

where n^a is the unit vector normal to Σ. Using the Einstein equation $G_{ab} = 8\pi T_{ab}$, Equation (1) transforms to

$$S_i(\Sigma) = -\int_{\Sigma}T^{ab}n_a(\phi_i)_b d\Sigma.$$

Let us use the 3+1 decomposition of the spacetime

$$ds^2 = -\alpha^2 d\eta^2 + a^2(t)\gamma_{ij}(dx^i + \beta^i d\eta)(dx^j + \beta^j d\eta). \tag{2}$$

We assume that the matter field is given by a single perfect fluid described by

$$T^{ab} = \rho u^a u^b + p(g^{ab} + u^a u^b), \tag{3}$$

where u^a is the four-velocity of the fluid element and that the background spacetime is given by a flat Friedmann–Lemaître–Robertson–Walker (FLRW) spacetime, in which the line element is written in the conformally flat form:

$$ds^2 = a^2(-d\eta^2 + dx^2 + dy^2 + dz^2).$$

We can naturally define ϕ_i^a, the generator of spatial rotation with respect to the peak of the density perturbation at $\boldsymbol{x} = \boldsymbol{x}_{pk}$, as

$$(\phi_i)^a = \epsilon_{ijk}(x - x_{pk})^j\delta^{kl}\left(\frac{\partial}{\partial x^l}\right)^a.$$

To the first order of perturbation from the flat FLRW spacetime, we find

$$S_i(\Sigma) = (1 + w)a^4\rho_b\epsilon_{ijk}\int_{\Sigma}(x - x_{pk})^j(v - v_{pk})^k d^3x$$

in the gauge with $\beta^k = 0$, where $v^i := u^i/u^0$, and we have assumed the equation of state $p = w\rho$. The region Σ should be taken as the region that will collapse into a black hole. Although the determination of Σ is a nontrivial task, following Heavens & Peacock (1988) and De Luca et al. (2019), we assume

$$\Sigma = \{\boldsymbol{x}|\delta(\boldsymbol{x}) > f\delta_{pk}\}. \tag{4}$$

We truncate the Taylor-series expansion of δ around the peak at the second order as

$$\delta \simeq \delta_{pk} + \frac{1}{2}\zeta_{ij}(x - x_{pk})^i(x - x_{pk})^j,$$

where

$$\zeta_{ij} := \left.\frac{\partial^2\delta}{\partial x^i\partial x^j}\right|_{\boldsymbol{x}=\boldsymbol{x}_{pk}}.$$

This truncation is justified provided that physical quantities do not change so steeply within Σ. Adjusting the x-, y-, and z-axes to the principal ones, we obtain

$$\delta \simeq \delta_{pk} - \frac{1}{2}\sigma_2\sum_{i=1}^{3}\lambda_i((x - x_{pk})^i)^2, \tag{5}$$

where σ_j and λ_i are defined in Appendix A. Equations (4) and (5) imply that Σ is given by an ellipsoid with the three axes given by

$$a_i^2 = 2\frac{\sigma_0}{\sigma_2}\frac{1 - f}{\lambda_i}\nu,$$

where we have defined $\nu := \delta_{pk}/\sigma_0$.

Taking the truncated Taylor-series expansion of $v - v_{pk}$ at $x = x_{pk}$,

$$v^i - v^i_{pk} \simeq v^i_j(x - x_{pk})^j,$$

we find

$$\begin{aligned} S_i(\Sigma) &\simeq (1 + w)a^4\rho_b\epsilon_{ijk}v_l^k\int_{\Sigma}(x - x_{pk})^j(x - x_{pk})^l d^3x \\ &= (1 + w)a^4\rho_b\epsilon_{ijk}v_l^k J^{jl}, \end{aligned} \tag{6}$$

where

$$\begin{aligned} v_l^k &:= \left.\frac{\partial v^k}{\partial x^l}\right|_{\boldsymbol{x}=\boldsymbol{x}_{pk}}, \\ J^{jl} &:= \int_{\Sigma}(x - x_{pk})^j(x - x_{pk})^l d^3x \\ &= \frac{4\pi}{15}a_1a_2a_3\ \mathrm{diag}\ (a_1^2, a_2^2, a_3^2). \end{aligned}$$

Here we concentrate on a growing mode of linear scalar perturbation, which is briefly summarized in Appendix B. According to peak theory (Bardeen et al. 1986; Heavens & Peacock 1988), which is briefly introduced in Appendix A, the distribution of the nondiagonal components of v_{ij} is independent of that of the trace-free part of J^{jl}. Then, we obtain

$$\sqrt{\langle S_i S^i\rangle} = S_{\mathrm{ref}}\sqrt{\langle s_e^i s_{ei}\rangle}, \tag{7}$$

where

$$S_{\mathrm{ref}}(\eta) = (1 + w)a^4\rho_b g(\eta)(1 - f)^{5/2}R_*^5, \tag{8}$$

$$\boldsymbol{s}_e = \frac{16\sqrt{2}\pi}{135\sqrt{3}}\left(\frac{\nu}{\gamma}\right)^{5/2}\frac{1}{\sqrt{\Lambda}}(-\alpha_1\tilde{v}_{23},\ \alpha_2\tilde{v}_{13},\ -\alpha_3\tilde{v}_{12}), \tag{9}$$

$$\alpha_1 = \frac{1}{\lambda_3} - \frac{1}{\lambda_2}, \quad \alpha_2 = \frac{1}{\lambda_3} - \frac{1}{\lambda_1}, \quad \alpha_3 = \frac{1}{\lambda_2} - \frac{1}{\lambda_1}, \quad \Lambda := \lambda_1\lambda_2\lambda_3, \tag{10}$$

and R_* and γ are defined in Appendix A. The quantity γ must satisfy $0 \leqslant \gamma \leqslant 1$, and we can usually assume $0.8 \lesssim \gamma \leqslant 1$ for PBH formation (De Luca et al. 2019). The function $g(\eta)$ is defined by

$$\langle (v_l^k(\eta))^2 \rangle = g^2(\eta) \langle (\tilde{v}_l^k)^2 \rangle \tag{11}$$

for all (k,l), where $\tilde{v}_l^k$ is time independent and defined in Equation (A3).[6]

2.2. Long-wavelength Solutions and Near-spherical Approximation

Motivated by inflationary cosmology, we consider cosmological long-wavelength solutions as initial data at $\eta = \eta_{\rm init}$, in which the density perturbation in the constant mean curvature (CMC) slicing is written in terms of the curvature perturbation ζ in the uniform-density slicing as follows (Harada et al. 2015):

$$\delta_{\rm CMC} = -\frac{1}{2\pi a^2 \rho_b} e^{5\zeta/2} \Delta e^{-\zeta/2}, \tag{12}$$

where $\Delta := \delta^{ij}\partial_i\partial_j$ and ζ is defined as $\gamma_{ij} = e^{-2\zeta}\delta_{ij}$ in the uniform-density slicing. We assume that the density perturbation is appropriately smoothed at scales smaller than the one under consideration. (See, e.g., Yoo et al. 2018, 2021; Young 2019; Tokeshi et al. 2020 for the possible dependence on the choice of window functions.)

To make the situation clear, we will apply peak theory to this density perturbation field. For $\nu \gg 1$, peak theory implies that the density perturbation is nearly spherical near the peak with $\lambda_i = (\gamma\nu/3)(1+\epsilon_i)$ (Bardeen et al. 1986; Heavens & Peacock 1988), where $\epsilon_i = O(1/(\gamma\nu))$, and hence we obtain

$$a_i \simeq r_f = \sqrt{6(1-f)}\frac{\sigma_0}{\sigma_1}. \tag{13}$$

That is, the region Σ is nearly spherical, and the deviation appears on the order of $1/\nu$.

In the following, we assume $w = 1/3$ and without loss of generality take $\boldsymbol{x}_{pk} = 0$. Linearizing Equation (12), we obtain

$$\delta_{\rm CMC} = \frac{2}{3a^2H_b^2}\Delta\zeta. \tag{14}$$

Therefore, we find

$$\sigma_j^2 = \frac{4}{9}\eta_{\rm init}^4 \int \frac{dk}{k} k^{4+2j} P_\zeta(k),$$

where we have assumed that $\zeta_{\boldsymbol{k}}(0)$ obeys a homogeneous Gaussian distribution with

$$\langle \zeta_{\boldsymbol{k}}(0)\zeta^*_{\boldsymbol{k}'}(0)\rangle = (2\pi)^3\delta^3(\boldsymbol{k}-\boldsymbol{k}')|\zeta_{\boldsymbol{k}}(0)|^2$$

and the power spectrum $P_\zeta(k)$ is defined as $P_\zeta(k) := k^3\,|\zeta_{\boldsymbol{k}}(0)|^2/(2\pi^2)$.

[6] In Heavens & Peacock (1988) and De Luca et al. (2019), the condition $v_l^k(\eta) = g(\eta)\tilde{v}_l^k$ is assumed.

As for the velocity gradient field, from Equation (B1), we have

$$v^i_j(\eta, \boldsymbol{x}) := \left(\frac{\partial v^i}{\partial x^j}\right)(\eta, \boldsymbol{x}) = \int \frac{d^3\boldsymbol{k}}{(2\pi)^3}\frac{k^i k_j}{k} v_{\boldsymbol{k}}(\eta) e^{i\boldsymbol{k}\cdot\boldsymbol{x}}. \tag{15}$$

Therefore, we obtain the following expression for $g(\eta)$,

$$g^2(\eta) = \frac{4}{9}\int \frac{dk}{k} k^2 T_v^2(k,\eta) P_\zeta(k), \tag{16}$$

where $T_v(k,\eta)$ is a transfer function for $v_{\boldsymbol{k}}(\eta)$ defined in Appendix B, and we have used $\langle \tilde{v}^i_j \tilde{v}^j_i \rangle = 1$ as seen in Equation (A1).

3. Estimate of the Angular Momentum

3.1. Narrow Power Spectrum

In general, we cannot expect a simple expression for $g(\eta)$ because it is obtained by a convolution of different modes with different time dependences. In Heavens & Peacock (1988), this is possible because the growth rate function is homogeneous at subhorizon scales in the Einstein–de Sitter universe. In De Luca et al. (2019), they implicitly assume that the perturbation of some single k effectively determines the angular momentum of the region Σ. Here, we assume the same assumption as in De Luca et al. (2019). This is possible if we assume the power spectrum has a narrow peak at $k = k_0$ so that

$$P_\zeta(k) \simeq \sigma_\zeta^2 k_0 \delta(k - k_0).$$

Then, Equation (14) implies

$$\sigma_j \simeq \frac{2}{3}\eta_{\rm init}^2 k_0^{2+j}\sigma_\zeta, \tag{17}$$

and therefore $\gamma \simeq 1$. In this case, from Equation (16), we can obtain

$$g(\eta) \simeq \frac{2}{3}k_0 |T_v(k_0,\eta)|\sigma_\zeta. \tag{18}$$

In a more general case, k_0 is identified with k, which dominates the integral on the right-hand side of Equation (16).

According to peak theory, in the case of a narrow power spectrum, the most probable profile is given by a sinc function (Bardeen et al. 1986; Yoo et al. 2018), that is,

$$\delta_{\rm CMC}(\eta, \boldsymbol{r}) = \delta_{pk}(\eta)\psi(r), \quad \zeta(\eta, \boldsymbol{r}) = \zeta_{pk}(\eta)\psi(r), \quad \psi(r) = \frac{\sin(k_0 r)}{k_0 r}.$$

Then, we can replace the harmonic function Y with $\psi(r)$. We identify $\delta_{pk}(\eta)$ with $\delta_{{\rm CMC},k_0}(\eta)$ in Equation (B2). From Equation (14), we obtain

$$\delta_{{\rm CMC},k_0}(\eta) \simeq \frac{2}{3}x^2(-\zeta_{k_0}(0)), \quad D = \frac{4\sqrt{3}}{3}(-\zeta_{k_0}(0)), \tag{19}$$

where $x = k_0\eta$ and D is defined in Appendix B.

3.2. PBH Formation Threshold

Under the truncated Taylor-series expansion, because the initial density perturbation profile is given by

$$\delta_{\mathrm{CMC},k_0}(\eta_{\mathrm{init}}, r) \simeq \delta_{\mathrm{CMC},k_0}(\eta_{\mathrm{init}})\left[1 - \frac{1}{6}(k_0 r)^2\right],$$

the compaction function $C_{\mathrm{CMC}}(\eta, r)$ in the CMC slicing is given in the long-wavelength limit by

$$C_{\mathrm{CMC}}(\eta_{\mathrm{init}}, r) := \left(\frac{\delta M}{ar}\right)(\eta_{\mathrm{init}}, r) \simeq \frac{1}{3}(k_0 r)^2\left[1 - \frac{1}{10}(k_0 r)^2\right](-\zeta_{k_0}(0)),$$

where δM is the mass excess. This is independent of η_{init}. It takes a maximum value C_{max} at $r = r_m$, where

$$C_{\mathrm{max}} = \frac{5}{6}(-\zeta_{k_0}(0)), \quad r_m = \sqrt{5}\, k_0^{-1}.$$

The threshold value of C_{max} for the PBH formation is known to $C_{\mathrm{max}} \simeq 0.38$–$0.42 \simeq 2/5$ from fully nonlinear numerical simulations, and this is fairly stable against different profiles of Gaussian-function or sinc-function shape (Shibata & Sasaki 1999; Harada et al. 2015; Germani & Musco 2019; Musco 2019). Using the threshold value $C_{\mathrm{max}} \simeq 2/5$, we can identify the threshold values for other variables as $\zeta_{k_0}(0) \simeq -12/25$ or $D \simeq 16\sqrt{3}/25$. For this value of $\zeta_{k_0}(0)$, we can calculate the density perturbation $\bar{\delta}_H$ averaged over the overdense region with the radius $r_0 = \sqrt{6}\, k_0^{-1}$ in the long-wavelength limit at horizon entry $\eta_{\mathrm{init}} = \eta_H$, which we define $(aH)(\eta_H) r_0 = 1$. The result is the following:

$$\bar{\delta}_H = \bar{\delta}(aHr_0)^2 \simeq \frac{2}{5} \cdot \frac{2}{3}(k_0 r_0)^2(-\zeta_{k_0}(0)) \simeq \frac{96}{125} = 0.768.$$

This is fairly consistent with the numerical value $\simeq$0.63–0.84 in the CMC slicing, which is obtained by converting the threshold value $\simeq$0.42–0.56 in the comoving slicing obtained in fully nonlinear numerical simulations for the Gaussian-function- or sinc-function-shaped profiles (Polnarev & Musco 2007; Musco & Miller 2013; Harada et al. 2015; Germani & Musco 2019; Musco 2019). Although the long-wavelength limit is only approximately valid at $\eta = \eta_H$, it is useful and conventional to use $\bar{\delta}_H$ obtained in the extrapolation of the long-wavelength limit to $\eta_{\mathrm{init}} = \eta_H$ to refer to the amplitude of the density perturbation. Alternatively, one can use the curvature perturbation $\zeta_{k_0}(0)$ for which the threshold and standard deviation are given by $\simeq -12/25$ and σ_ζ, respectively. From now on, if we set $\eta_{\mathrm{init}} = \eta_H$ in Equation (17), we denote σ_0 by σ_H. Then, we find

$$\sigma_H = 4\sigma_\zeta.$$

Using this notation, from Equation (18), we find

$$g(\eta) \simeq \frac{1}{6}|T_v(k_0, \eta)| k_0 \sigma_H. \tag{20}$$

We should note that because $\bar{\delta}$, the density perturbation averaged over the overdense region, is given by $\bar{\delta} \simeq (2/5)\delta_{pk}$, we find

$$\nu = \frac{\delta_{pk}}{\sigma_0} \simeq \frac{5}{2}\frac{\bar{\delta}_H}{\sigma_H} = \frac{5}{2}\bar{\nu},$$

where we have defined $\bar{\nu}$ as $\bar{\nu} = \bar{\delta}_H/\sigma_H$.

3.3. Decoupling from the Cosmological Expansion

In De Luca et al. (2019), the angular momentum of the region Σ at the horizon entry of the inverse wavenumber is identified with the initial spin angular momentum of the black hole by arguing that turnaround occurs immediately after the horizon entry. This might result in misestimating the nondimensional spin parameter because the angular momentum increases and the mass decreases in time during the cosmological expansion. Here, we will estimate the angular momentum of the black hole by that of the region Σ at turnaround, after which the evolution of the region decouples from the cosmological expansion, and the mass and the angular momentum of the collapsing region should be approximately conserved. However, it is not a trivial task to determine this moment. Strictly speaking, turnaround is beyond the regime of linear perturbation. However, because it can be regarded as still being in a quasi-linear regime, we should be able to apply an extrapolation of linear perturbation theory. We here identify the condition $\delta_{\mathrm{CMC}} \simeq 1$ in the CMC slicing as the decoupling condition because this implies that the local density perturbation becomes so large that the expansion should be about to turn around.

To go beyond the turnaround, CMC slicing will not be appropriate because the maximum expansion means a vanishing mean curvature, while there exists a far region where the mean curvature is nonvanishing due to Hubble expansion. To avoid this difficulty, we will shift to the conformal Newtonian gauge. It is expected that the dynamics should fit a usual Newtonian picture later. For this reason, we evaluate $T_v(\eta_{\mathrm{ta}})$ in Equation (16) for v_{CN}, the velocity perturbation in the conformal Newtonian gauge at the decoupling from the cosmological expansion.

In Figure 1, we can see that the turnaround occurs at $x = x_{\mathrm{ta}} \simeq 2.14$ for $D = 16\sqrt{3}/25$. The value of the transfer function at the turnaround $x = x_{\mathrm{ta}}$ is calculated to give

$$T_{v_{\mathrm{CN}}}(k_0, \eta_{\mathrm{ta}}) = \frac{v_{\mathrm{CN}}(x_{\mathrm{ta}})}{\Phi_{k_0}(0)} \simeq 0.622,$$

where we have used $v_{\mathrm{CN}}(x_{\mathrm{ta}}) \simeq -0.199$. Thus, from Equation (20), the value of $g_{\mathrm{CN}}(\eta_{\mathrm{ta}})$ is given by

$$g_{\mathrm{CN}}(\eta_{\mathrm{ta}}) \simeq 0.104 k_0 \sigma_H.$$

Although there is some ambiguity in the choice of the decoupling condition and the gauge condition, it will not change the estimate by orders of magnitude as seen from Figure 1 if we choose x_{ta} between $\simeq$1.5 and $\simeq$3.

4. Estimate of the Nondimensional Kerr Parameter

4.1. Estimate of A_{ref}

Let us estimate the reference spin value at turnaround:

$$A_{\mathrm{ref}}(\eta_{\mathrm{ta}}) = \frac{S_{\mathrm{ref}}(\eta_{\mathrm{ta}})}{GM_{\mathrm{ta}}^2} = \frac{\frac{4}{3}[a^4 \rho_b g_{\mathrm{CN}}](\eta_{\mathrm{ta}})(1-f)^{5/2} R_*^5}{GM_{\mathrm{ta}}^2}, \tag{21}$$

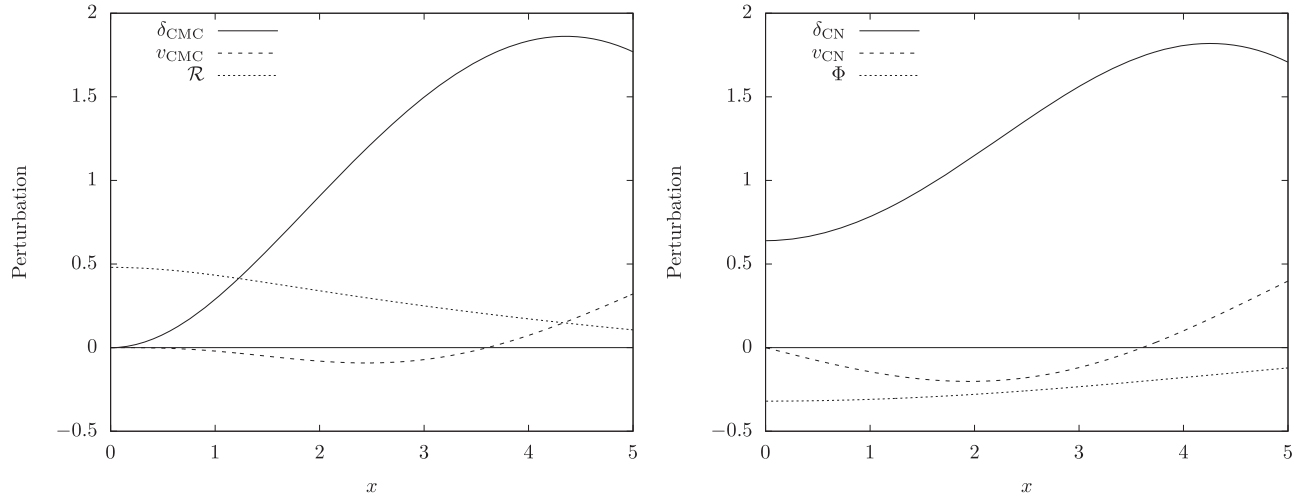

Figure 1. The functions $v_{\rm CMC}$, $\delta_{\rm CMC}$, and $\mathcal{R}$ in the CMC slicing and $\delta_{\rm CN}$, $v_{\rm CN}$, and Φ in the conformal Newtonian gauge are plotted for $D = 16\sqrt{3}/25$ as functions of $x = k\eta$. We can see that $\delta_{\rm CMC}$ gets larger than unity at $x \simeq 2.14$, at which $v_{\rm CN} \simeq -0.199$.

where the black hole mass M is identified with the mass within the region Σ at turnaround,

$$M_{\rm ta} = (\rho_b a^3)(\eta_{\rm ta}) \cdot \frac{4}{3}\pi r_f^3.$$

This is different from M_H, which we define to be the mass within the horizon at the horizon entry of the overdense region. The condition for the horizon entry $H^{-1}(\eta_H) = ar_0$ implies $\eta_H = r_0$ or $x = \sqrt{6}$. Because $a(\eta) \propto \eta$, we have

$$\frac{a(\eta_{\rm ta})}{a(\eta_H)} = \frac{\eta_{\rm ta}}{r_0} = \frac{x_{\rm ta}}{\sqrt{6}}.$$

Using $\rho_b a^3 \propto a^{-1}$, we find

$$M_{\rm ta} \simeq \frac{\sqrt{6}}{x_{\rm ta}}(1-f)^{3/2} M_H.$$

Using Equation (20) and $2GM_H = a(\eta_H) r_0$, we obtain a simple expression:

$$A_{\rm ref}(\eta_{\rm ta}) \simeq \frac{1}{24\sqrt{3}\,\pi} x_{\rm ta}^2 (1-f)^{-1/2} |T_{v_{\rm CN}}(k_0, \eta_{\rm ta})| \sigma_H. \quad (22)$$

4.2. Estimate of a_*

As for the distribution of s_e, we just quote the result of Heavens & Peacock (1988) with the correction by De Luca et al. (2019). For the large ν limit, if we define h by

$$s_e := \sqrt{\boldsymbol{s}_e \cdot \boldsymbol{s}_e} = \frac{2^{9/2}\pi}{5\gamma^6 \nu}\sqrt{1-\gamma^2}\, h,$$

the probability distribution of h is approximately given by

$$P(h)dh \simeq \exp\left[-2.37 - 4.12 \ln h - 1.53(\ln h)^2 - 0.13(\ln h)^3\right] dh.$$

$P(h)$ takes a maximum at $h \simeq 0.178$, while $\sqrt{\langle h^2 \rangle} \simeq 0.419$. Using

$$P(s_e|\nu) ds_e = P(h) \frac{dh}{ds_e} ds_e,$$

we have

$$\sqrt{\langle s_e^2 \rangle} \simeq 5.96 \frac{\sqrt{1-\gamma^2}}{\gamma^6 \nu}.$$

Putting $a = A_{\rm ref} s_e = Ch$, we have

$$P_a(a) da = P(C^{-1}a) C^{-1} da.$$

From the above argument and the equation

$$\sqrt{\langle a_*^2 \rangle} = A_{\rm ref}(\eta_{\rm ta}) \sqrt{\langle s_e^2 \rangle},$$

we find the expression for the initial spin of PBHs for $\gamma \simeq 1$:

$$\sqrt{\langle a_*^2 \rangle} \simeq \frac{5.96}{24\sqrt{3}\,\pi} x_{\rm ta}^2 (1-f)^{-1/2} T_{v_{\rm CN}}(k_0, \eta_{\rm ta}) \sigma_H \sqrt{1-\gamma^2}\, \nu^{-1}. \quad (23)$$

Putting $x_{\rm ta} = 2.14$, $T_{v_{\rm CN}}(k_0, \eta_{\rm ta}) = 0.622$, $\bar{\delta}_H = \bar{\nu}\sigma_H$, $\nu = (5/2)\bar{\nu}$, and $\bar{\delta}_H \simeq 0.768$, we find

$$\sqrt{\langle a_*^2 \rangle} \simeq 3.90 \times 10^{-3} (1-f)^{-1/2} \sqrt{1-\gamma^2} \left(\frac{\nu}{8}\right)^{-2} \quad (24)$$

for the PBH mass

$$M \simeq 1.14(1-f)^{3/2} M_H. \quad (25)$$

Eliminating f from Equations (24) and (25), we obtain the following simple expression:

$$\sqrt{\langle a_*^2 \rangle} \simeq 4.01 \times 10^{-3} \left(\frac{M}{M_H}\right)^{-1/3} \sqrt{1-\gamma^2} \left(\frac{\nu}{8}\right)^{-2}. \quad (26)$$

Although f or M is a free parameter in the present scheme, numerical simulations strongly suggest $M \simeq M_H$ except for the near-critical case in which $M \ll M_H$ (Musco & Miller 2013; Escrivà 2020). If we put $M = M_H$, $\gamma = 0.85$, and $\boldsymbol{\nu} = 8$, the above expression yields $\sqrt{\langle a_*^2 \rangle} \simeq 2.14 \times 10^{-3}$. Therefore, we conclude that $\sqrt{\langle a_*^2 \rangle} = O(10^{-3})$ or even smaller for $M \simeq M_H$.

Let us now discuss small PBHs formed in the near-critical case. In this case, only a small fraction of PBHs are produced through critical collapse, while the rest have $M \sim M_H$. Therefore, we should fix ν at the scale of M_H. Using Equation (26), for example, we find $\sqrt{\langle a_*^2 \rangle} \simeq 2.14 \times 10^{-2}$ for $M = 10^{-3} M_H$,

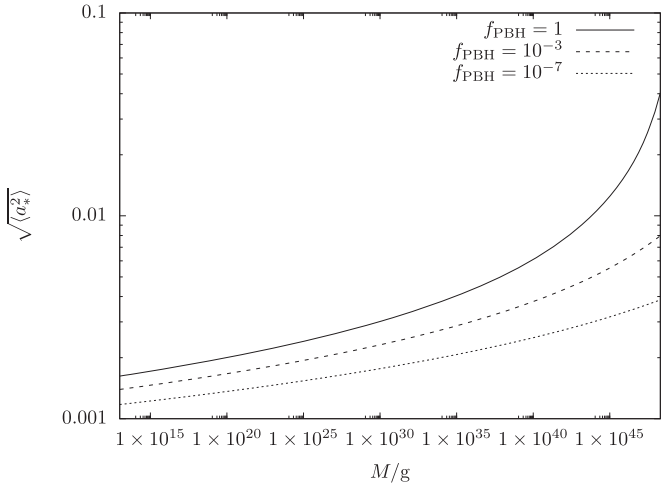

Figure 2. The standard deviation of the initial spins of the PBH, $\sqrt{\langle a_*^2 \rangle}$, as a function of the PBH mass M with fixed $f_{\rm PBH}$, where we have assumed that the PBH mass is equal to the horizon mass, i.e., $M = M_H$ and $\gamma = 0.85$.

$\gamma = 0.85$, and $\bar{\nu} = 8$. It also strongly suggests that the angular momentum will play an important role and may significantly suppress the formation of PBHs of $M \lesssim 10^{-8} M_H$, for which $\sqrt{\langle a_*^2 \rangle} \gtrsim 1$.

4.3. Implications

Because our expression is given in terms of ν, the initial spin directly depends on the fraction $\beta_0(M_H)$ of the universe that collapsed into black holes. If we use the Press–Schechter approximation as a rough estimate of $\beta_0(M_H)$ (Carr 1975),

$$\beta_0(M_H) \simeq \sqrt{\frac{2}{\pi}} \frac{1}{\nu_{\rm th}} e^{-\nu_{\rm th}^2/2} = \sqrt{\frac{2}{\pi}} \frac{2}{5} \frac{\sigma_H}{\bar{\delta}_{H,\rm th}} \exp\left[-\left(\frac{5}{2}\right)^2 \frac{\bar{\delta}_{H,\rm th}^2}{2\sigma_H^2} \right],$$

we find a simple expression

$$\sqrt{\langle a_*^2 \rangle} \simeq 4.01 \times 10^{-3} \left(\frac{M}{M_H}\right)^{-1/3} \sqrt{1-\gamma^2} \times \left[1 - 0.072 \log_{10}\left(\frac{\beta_0(M_H)}{1.3 \times 10^{-15}} \right) \right]^{-1},$$

where $\boldsymbol{\nu}$ is identified with $\boldsymbol{\nu}_{\rm th}$ and a weak dependence on $\boldsymbol{\nu}_{\rm th}$ in the logarithm is ignored. For simplicity, let us concentrate on PBHs of $M \simeq M_H$. Using the relation between $\beta_0(M)$ and $f_{\rm PBH}(M)$ (Carr et al. 2010),

$$\Omega_{\rm dm} f_{\rm PBH}(M) \simeq 10^{18} \beta_0(M) \left(\frac{M}{10^{15}\ \mathrm{g}} \right)^{-1/2},$$

we further obtain

$$\sqrt{\langle a_*^2 \rangle} \simeq 4.01 \times 10^{-3} \times \frac{\sqrt{1-\gamma^2}}{1 + 0.036 \left[21 - 2 \log_{10}\left(\frac{f_{\rm PBH}(M)}{10^{-7}} \right) - \log_{10}\left(\frac{M}{10^{15}\ \mathrm{g}} \right) \right]}. \quad (27)$$

We plot Equation (27) in Figure 2. In this figure, we can see that the larger $f_{\rm PBH}(M)$ and M are, the larger $\sqrt{\langle a_*^2 \rangle}$. For example, $\sqrt{\langle a_*^2 \rangle}$ of PBHs for $M = 50 M_\odot$ and $f_{\rm PBH} = 1$ is about 3.3 times larger than that for $M = 10^{15}$ g and $f_{\rm PBH} = 10^{-7}$.

5. Summary and Discussion

We have applied Heavens & Peacock's (1988) approach to the first-order effect on the spins of PBHs. Although we have presented numerical values with two or three significant digits, at present we admit that there is large uncertainty in modeling PBH formation. Nevertheless, we would like to claim that the standard deviation of the initial spins is given by $\sqrt{\langle a_*^2 \rangle} = O(10^{-3})$ or even smaller for $M \simeq M_H$ based on peak theory. We have obtained the expression

$$\sqrt{\langle a_*^2 \rangle} \simeq 4.0 \times 10^{-3} \left(\frac{M}{M_H}\right)^{-1/3} \sqrt{1-\gamma^2} \left(\frac{\nu_{\rm th}}{8}\right)^{-2} \simeq 4.0 \times 10^{-3} \left(\frac{M}{M_H}\right)^{-1/3} \sqrt{1-\gamma^2} \times \left[1 - 0.072 \log_{10}\left(\frac{\beta_0(M_H)}{1.3 \times 10^{-15}} \right) \right]^{-1}.$$

The above formula also implies that the higher the PBH formation probability $\beta_0(M_H)$, the larger the standard deviation of the spins. On the other hand, for PBHs of $M \ll M_H$ in the near-critical case, we find that $\sqrt{\langle a_*^2 \rangle}$ can be much larger than that for PBHs of $M \simeq M_H$.

In comparison to the expression in De Luca et al. (2019), the new estimate has no overall factor $\Omega_{\rm dm}$, takes critical collapse into consideration, and gives an explicit expression in terms of $\beta_0(M_H)$. The proof of the nonexistence of the overall factor $\Omega_{\rm dm}$ is delegated to Appendix C. From a physical point of view, dark matter does not play any role in dynamics well into the radiation-dominated phase. On the other hand, their assumption that turnaround occurs almost simultaneously with the horizon entry is supported if we take the horizon entry not of the inverse wavenumber but of the radius of the overdense region. As for the gauge choice, we have taken the conformal Newtonian gauge to evaluate the angular momentum at turnaround. If we instead continued taking the CMC slicing as in De Luca et al. (2019), the estimate would be further reduced by approximately half as seen in Figure 1.

Here, we would like to compare the present result with PBHs formed in the matter-dominated phase of the universe. As seen in this paper, in the radiation-dominated phase, because $\nu_{\rm th}$ is large as suggested by the Jeans argument, peak theory implies that the region Σ is nearly spherical and the effect of tidal torque is suppressed. In fact, as we can see in Equation (9), only the trace-free part $\mathcal{J}^{jl}$ of J^{jl} enters the expression of the angular momentum, and we can see that $\sqrt{\langle (\mathcal{J}^{jl}\mathcal{J}_{jl})/(J^{jl}J_{jl}) \rangle} = O(\nu^{-1})$ for large ν and also $g(\eta) \sim k_0 \sigma_H$. In the matter-dominated phase, because $\nu_{\rm th}$ is vanishingly small in spherical symmetry, the region Σ can be far from spherical and the tidal torque can give the large amount of angular momentum on Σ. Therefore, it is predicted that the angular momentum within the region Σ is so large that PBH formation can be strongly suppressed and that the PBHs formed can have near-extremal spins (Harada et al. 2017). This suggests that for PBHs that formed in the phase transition at which the equation of state is softer than the radiation, their

spins can be larger than those formed in the radiation-dominated phase.

It would be interesting to remove the assumption of a narrow power spectrum as the broad mass function of PBHs is intensively discussed from an observational point of view (Carr et al. 2016; Carr & Kühnel 2019), although the deviation of γ from unity might not change the result by orders of magnitude. Note also that although we have investigated the first-order effect on the angular momentum, the obtained result is apparently second order in terms of σ_H as we can see in Equations (23) and (24), where ν^{-1} and $\bar{\nu}^{-1}$ are of the order of σ_H because the threshold value of the PBH formation for the perturbation amplitude is of the order of unity. This means that the first-order effect investigated here might be comparable to the second-order effect. In fact, in Mirbabayi et al. (2020), the second-order effect is estimated to be $\sqrt{\langle a_*^2\rangle} \simeq \langle\zeta^2\rangle$. Finally, it should be noted that our analysis is based on linear perturbation theory, which is not completely justified for perturbations that can generate PBHs. In particular, the behaviors of the solutions at the final stage of black hole formation are highly nonlinear and cannot be predicted by linear perturbation theory. Along this line, the assumption of the conservation of the nondimensional Kerr parameter after the decoupling from the cosmological expansion should be confirmed by numerical simulations. It is clear that further investigations are necessary to answer the problem of how large PBH spins are.

T.H. is very grateful to B. J. Carr for introducing this problem to him. T.H. would also like to thank T. Murata, K. Nakashi, T. Sato, and Y. Watanabe for interesting discussions on peak theory. The authors would like to thank K. Nakao for his helpful comment and continuous encouragement. They would also like to thank the anonymous referee for the important comments and suggestions. This work was supported by JSPS KAKENHI grant Nos. JP19H01895 (T.H. and C.Y.), JP19K03876 (T.H.), JP17H01131 (K.K.), and JP19J12007 (Y. K.) and MEXT KAKENHI grant Nos. JP19H05114 (K.K.) and JP20H04750 (K.K.).

Appendix A
Peak Theory

We briefly review peak theory based on Heavens & Peacock (1988). We treat the following fields as probability variables:

$$\delta, \quad \zeta_i = \frac{\partial\delta}{\partial x^i}, \quad \zeta_{ij} = \frac{\partial^2\delta}{\partial x_i \partial x_j}, \quad v^i_j = \frac{\partial v^i}{\partial x^j}.$$

The correlations of the above variables are given by

$$\begin{aligned}
&\langle\delta^2\rangle = \sigma_0^2, \quad \langle\delta\zeta_{11}\rangle = -\langle\zeta_1\zeta_1\rangle = \cdots = -\frac{\sigma_1^2}{3},\\
&\langle\delta\tilde{v}_{11}\rangle = \cdots = -\frac{\sigma_0}{3},\\
&\langle\zeta_{11}^2\rangle = 3\langle\zeta_{11}\zeta_{22}\rangle = 3\langle\zeta_{12}^2\rangle = \cdots = \frac{\sigma_2^2}{5},\\
&\langle\zeta_{11}\tilde{v}_{11}\rangle = 3\langle\zeta_{11}\tilde{v}_{22}\rangle = 3\langle\zeta_{12}\tilde{v}_{12}\rangle = \cdots = \frac{\sigma_1^2}{5\sigma_0},\\
&\langle\tilde{v}_{11}^2\rangle = 3\langle\tilde{v}_{11}\tilde{v}_{22}\rangle = 3\langle\tilde{v}_{12}^2\rangle = \cdots = \frac{1}{5},
\end{aligned} \tag{A1}$$

and all other correlations vanish, where

$$\sigma_j^2 := \int \frac{d^3\boldsymbol{k}}{(2\pi)^3} k^{2j}|\delta_{\boldsymbol{k}}|^2, \tag{A2}$$

$$\tilde{v}^i_j := -\frac{1}{\sigma_0}\int \frac{d^3\boldsymbol{k}}{(2\pi)^3}\frac{k^i k_j}{k^2}\delta_{\boldsymbol{k}} e^{i\boldsymbol{k}\cdot\boldsymbol{x}}. \tag{A3}$$

Putting the eigenvalues of $-\zeta_{ij}/\sigma_2$ as λ_1, λ_2, and λ_3 ($\lambda_1 \geqslant \lambda_2 \geqslant \lambda_3$), and

$$\begin{aligned}
&\nu = \delta/\sigma_0, \quad \xi_1 = \lambda_1 + \lambda_2 + \lambda_3, \quad \xi_2 = \frac{1}{2}(\lambda_1 - \lambda_3),\\
&\xi_3 = \frac{1}{2}(\lambda_1 - 2\lambda_2 + \lambda_3),\\
&w_1 = \tilde{v}_{23}, \quad w_2 = \tilde{v}_{13}, \quad w_3 = \tilde{v}_{12},
\end{aligned}$$

the probability distribution of ν, $\boldsymbol{\lambda}$, and $\boldsymbol{w}$ at a peak is given by

$$N_{pk}(\nu, \boldsymbol{\lambda}, \boldsymbol{w})d\nu d^3\boldsymbol{\xi} d\boldsymbol{w} = \frac{B}{R_*^3}\exp(-Q_4)F(\boldsymbol{\lambda})d\nu d^3\boldsymbol{\lambda} d^3\boldsymbol{w},$$

where

$$\begin{aligned}
&B = \frac{3^{9/2}5^4}{2^{11/2}\pi^{9/2}(1-\gamma^2)^2},\\
&2Q_4 = \nu^2 + \frac{(\xi_1 - \gamma\nu)^2}{1-\gamma^2} + 15\xi_2^2 + 5\xi_3^2 + 15\frac{w_1^2 + w_2^2 + w_3^2}{1-\gamma^2},\\
&F(\boldsymbol{\lambda}) = \frac{27}{2}\lambda_1\lambda_2\lambda_3(\lambda_2 - \lambda_3)(\lambda_1 - \lambda_3)(\lambda_1 - \lambda_2),\\
&R_* := \sqrt{3}\frac{\sigma_1}{\sigma_2}, \quad \gamma := \sigma_1^2/(\sigma_0\sigma_2),
\end{aligned}$$

We can see that the distribution of $\boldsymbol{w}$ is independent from other variables.

Appendix B
Cosmological Linear Perturbations

Here we briefly review the result of cosmological linear perturbation theory that is necessary for the present paper. We basically follow the notation of Kodama & Sasaki (1984). We would like readers to refer to Kodama & Sasaki (1984) or other reference for the derivation. The scalar, vector, and tensor harmonic functions Y, Y_i, Y_{ij} in flat space for scalar perturbations are defined as follows:

$$\begin{aligned}
&Y = Ce^{ik_l x^l}, \quad Y_i = -k^{-1}Y_{|i}, \quad Y_{ij} = k^{-2}\left(Y_{|ij} - \frac{1}{3}\delta_{ij}\Delta Y\right)\\
&\quad = -\left(\frac{k_i k_j}{k^2} - \frac{1}{3}\delta_{ij}\right)Y,
\end{aligned}$$

where the roman indices are raised and lowered by δ^{ij} and δ_{ij}, respectively, and Y satisfies

$$(\Delta + k^2)Y = 0.$$

The Fourier decomposition of the perturbations is given by

$$\delta(\eta, \boldsymbol{x}) = \int \frac{d^3\boldsymbol{k}}{(2\pi)^3}\delta_{\boldsymbol{k}}(\eta)e^{i\boldsymbol{k}\cdot\boldsymbol{x}}, \quad \delta_{\boldsymbol{k}}(\eta) = \int d^3\boldsymbol{x}\delta(\eta, \boldsymbol{x})e^{-i\boldsymbol{k}\cdot\boldsymbol{x}},$$

and so on. In what follows in this section, we abbreviate $\delta_{\boldsymbol{k}}(\eta)$ as δ and so on. In Equation (2), we write the scalar perturbation

of the metric tensor as follows:

$$\alpha = a(1 + AY), \quad \beta_i = -a^2 BY_i, \quad \gamma_{ij} = \delta_{ij} + 2H_L Y\delta_{ij} + 2H_T Y_{ij}.$$

The trace of the extrinsic curvature of the constant η hypersurface is written as

$$K = K_b(1 + \mathcal{K}_g Y).$$

The perturbed quantities of the perfect fluid are written as

$$\rho = \rho_b(1 + \delta Y), \quad p = p_b(1 + \pi_L Y), \quad v^i = \frac{u^i}{u^0} = vY^i. \tag{B1}$$

In the adiabatic process with the $p = w\rho$ equation of state, we have $\pi_L = \delta$. For the scalar perturbation, the infinitesimal coordinate transformation is given by

$$\bar{\eta} = \eta + T(\eta)Y, \quad \bar{x}^j = x^j + L(\eta)Y^j,$$

where T and L are arbitrary functions of η. Under this coordinate transformation, the metric perturbation quantities transform as follows:

$$\overline{A} = A - T' - \mathcal{H}T, \quad \overline{B} = B + L' + kT,$$
$$\overline{H_L} = H_L - \frac{k}{n}L - \mathcal{H}T, \quad \overline{H_T} = H_T + kL,$$

where n is the dimension of the space, $\mathcal{H} := a'/a$, and the prime denotes the derivative with respect to η. On the other hand, matter perturbation quantities transform as follows:

$$\bar{v} = v + L', \quad \bar{\delta} = \delta + n(1 + w)\mathcal{H}T,$$
$$\bar{\pi}_L = \pi_L + 3\frac{c_s^2}{w}(1 + w)\mathcal{H}T,$$

where $c_s^2 = w$ is the sound speed. From the above, we can construct gauge-invariant perturbation quantities corresponding to δ and V as follows:

$$\Delta = \delta + 3(1 + w)\mathcal{H}k^{-1}(v - B), \quad V = v - k^{-1}H_T'.$$

From the Einstein equation, we can derive the equations for the gauge-invariant variables Δ and V. We present the solutions for the radiation-dominated phase of the universe below:

$$\Delta(x) = D\sqrt{3}\left(\frac{\sin z}{z} - \cos z\right),$$
$$V(x) = D\left[\frac{3}{4}\left(\frac{2}{z^2} - 1\right)\sin z - \frac{3}{2}\frac{\cos z}{z}\right],$$

where D is an arbitrary constant, $z := x/\sqrt{3}$, $x := k\eta$, and a decaying mode is omitted.

In the CMC ($\mathcal{K}_g = 0$) slicing with $B = 0$, using the above solutions for $\Delta(x)$ and $V(x)$, we can obtain

$$\delta = D\frac{\sqrt{3}z^2}{z^2 + 2}\left(2\frac{\sin z}{z} - \cos z\right), \tag{B2}$$

$$v = -\frac{3}{4}D\frac{(z^2 - 2)\sin z + 2z\cos z}{z^2 + 2}, \tag{B3}$$

$$\mathcal{R} = D\frac{\sqrt{3}}{2}\frac{1}{z^2 + 2}\left(2\frac{\sin z}{z} - \cos z\right), \tag{B4}$$

where $\mathcal{R} = H_L + \frac{1}{3}H_T$. In this gauge, A and $\mathcal{R}$ are completely fixed, while H_T and H_L are fixed only up to a constant.

In the conformal Newtonian gauge, in which $H_T = B = 0$, we can obtain

$$\delta = \sqrt{3}D\frac{2(z^2 - 1)\sin z + (2 - z^2)z\cos z}{z^3}, \tag{B5}$$

$$v = \frac{3}{4}D\frac{(2 - z^2)\sin z - 2z\cos z}{z^2}, \tag{B6}$$

$$\Phi = -\frac{\sqrt{3}}{2}D\frac{\sin z - z\cos z}{z^3}, \tag{B7}$$

where $H_L = -\Phi$ and $A = \Phi$. Thus, all perturbation quantities are completely fixed in this gauge.

We can define the transfer functions $T_{\delta_{\rm CMC}}$, $T_{v_{\rm CMC}}$, $T_{\delta_{\rm CN}}$, and $T_{v_{\rm CN}}$ as follows:

$$\delta_{\rm CMC}(\eta) = T_{\delta_{\rm CMC}}(k, \eta)\Phi(0), \quad v_{\rm CMC}(\eta) = T_{v_{\rm CMC}}(k, \eta)\Phi(0),$$
$$\delta_{\rm CN}(\eta) = T_{\delta_{\rm CN}}(k, \eta)\Phi(0), \quad v_{\rm CN}(\eta) = T_{v_{\rm CN}}(k, \eta)\Phi(0),$$

where we can see $\Phi(0) = -D/(2\sqrt{3}) = -(2/3)\mathcal{R}(0)$ from Equations (B4) and (B7). We should note that $\mathcal{R}(0) = -\zeta(0)$, where ζ is the curvature perturbation in the uniform-density slicing.

Appendix C
Nonexistence of the Overall Factor $\Omega_{\rm dm}$

Here, we show that the overall factor $\Omega_{\rm dm}$ in De Luca et al.'s (2019) expression should be removed. Although their notation is slightly different from ours, we consistently continue to use our notation.

In the following, we follow the process of calculation in De Luca et al. (2019). They estimate the angular momentum at the horizon entry of the inverse wavenumber, saying that the turnaround is just after the horizon entry. Their analysis is confined to the CMC slicing, where $g(\tilde{\eta}_H) = g_{\rm CMC}(\tilde{\eta}_H)$ was estimated to be

$$g_{\rm CMC}(\tilde{\eta}_H) \sim \left|\frac{T_{v_{\rm CMC}}(k_0, \tilde{\eta}_H)}{T_{\delta_{\rm CMC}}(k_0, \tilde{\eta}_H)}\right| k_0\tilde{\sigma}_H, \tag{C1}$$

where k_0 is identified with k_H in De Luca et al. (2019), $\tilde{\eta}_H = k_0^{-1}$, and $\tilde{\sigma}_H$ is σ_0 at $\eta = \tilde{\eta}_H$ without the long-wavelength limit. Although our calculation does not reproduce their numerical value $|T_{v_{\rm CMC}}(k_0, \tilde{\eta}_H)/T_{\delta_{\rm CMC}}(k_0, \tilde{\eta}_H)| \sim 0.5$ but gives a much smaller value $\simeq 0.0714$ at $x = 1$, this is not the origin of the factor $\Omega_{\rm dm}$. Because $\mathcal{H} \propto a^{-1}$ in the radiation-dominated era and $\mathcal{H} \propto a^{-1/2}$ in the matter-dominated era, they probably inferred that

$$\mathcal{H}(\eta_{\rm eq}) = \frac{\mathcal{H}_0}{(a(\eta_{\rm eq})/a_0)^{1/2}}, \tag{C2}$$

where we have put $a(\eta_0) = a_0$ and $\mathcal{H}(\eta_0) = \mathcal{H}_0$ and η_0 is the present conformal time. This corresponds to Equation (5.4) in De Luca et al. (2019). Then, using

$$\frac{a(\tilde{\eta}_H)}{a_0} = \frac{a(\eta_{\rm eq})}{a_0}\left(\frac{\mathcal{H}(\eta_{\rm eq})}{\mathcal{H}(\tilde{\eta}_H)}\right) = \left(\frac{a(\eta_{\rm eq})}{a_0}\right)^{1/2}\left(\frac{\mathcal{H}_0}{\mathcal{H}(\tilde{\eta}_H)}\right) \tag{C3}$$

and defining $\tilde{M}_H$ as the mass within the Hubble horizon at $\eta = \tilde{\eta}_H$, we find

$$\mathcal{H}(\tilde{\eta}_H) = \frac{a(\tilde{\eta}_H)}{2G\tilde{M}_H} = \left(\frac{a(\eta_{\rm eq})}{a_0}\right)^{1/2} \frac{\mathcal{H}_0}{\mathcal{H}(\tilde{\eta}_H)} \frac{a_0}{2G\tilde{M}_H} \tag{C4}$$

and

$$k_0 = \left(\frac{a(\eta_{\rm eq})}{a_0}\right)^{1/4} \sqrt{\frac{\mathcal{H}_0 a_0}{2G\tilde{M}_H}}. \tag{C5}$$

Moreover, using

$$\rho_b(\tilde{\eta}_H)\left(\frac{a(\tilde{\eta}_H)}{a_0}\right)^4 \simeq \rho_{\rm rad}(\tilde{\eta}_H)\left(\frac{a(\tilde{\eta}_H)}{a_0}\right)^4$$
$$\simeq \rho_{\rm rad}(\eta_0) = \Omega_{\rm dm}\frac{a(\eta_{\rm eq})}{a_0}\frac{3\mathcal{H}_0^2}{8\pi G a_0^2},$$
$$k_0^{-1} = \mathcal{H}^{-1}(\tilde{\eta}_H) = \frac{2G\tilde{M}_H}{a(\tilde{\eta}_H)}$$

and identifying the mass of the PBH with $\tilde{M}_H$, they reached their conclusion:

$$A_{\rm ref,CMC}(\tilde{\eta}_H) \simeq \frac{\frac{4}{3}a_0^4\Omega_{\rm dm}\frac{a(\eta_{\rm eq})}{a_0}\frac{3\mathcal{H}_0^2}{8\pi G a_0^2}\frac{1}{2}\left[\left(\frac{a(\eta_{\rm eq})}{a_0}\right)^{1/4}\sqrt{\frac{\mathcal{H}_0 a_0}{2G\tilde{M}_H}}\right]^{-4}\tilde{\sigma}_H}{G\tilde{M}_H^2} \simeq \frac{\Omega_{\rm dm}}{\pi}\tilde{\sigma}_H, \tag{C6}$$

where $g_{\rm CMC}(\tilde{\eta}_H) \sim 0.5 k_0 \tilde{\sigma}_H$, $R_* \simeq \sqrt{3}\,k_0^{-1}$, and $1 - f \simeq 1/3$ have been used.

In the following, we would like to redo the above estimate more carefully. Let us keep $g_{\rm CMC}(\tilde{\eta}_H)$ as in Equation (C1) and focus on the factor $\Omega_{\rm dm}$. Using $\tilde{M}_H = (4\pi/3)(\rho_b a^3)(\tilde{\eta}_H)(k_0^{-1})^3$, we can directly get the following simple estimate:

$$A_{\rm ref,CMC}(\tilde{\eta}_H) = \frac{\frac{4}{3}[a^4\rho_b g_{\rm CMC}](\tilde{\eta}_H)(1-f)^{5/2}R_*^5}{G\tilde{M}_H^2} \simeq 2\left|\frac{T_{\nu_{\rm CMC}}(k_0, \tilde{\eta}_H)}{T_{\delta_{\rm CMC}}(k_0, \tilde{\eta}_H)}\right|\frac{\tilde{\sigma}_H}{\pi}, \tag{C7}$$

where we have used the Friedmann equation only at the formation of PBHs well in the radiation-dominated era. We can see that there is no overall factor $\Omega_{\rm dm}$.

Although the above derivation is complete, it might be useful to trace the calculation in De Luca et al. (2019) in the right way. Assuming that the energy of the universe consists of radiation, dark matter, and the cosmological constant, the Friedmann equation implies

$$H^2 = H_0^2\left[\Omega_{\rm rad}\left(\frac{a_0}{a}\right)^4 + \Omega_{\rm dm}\left(\frac{a_0}{a}\right)^3 + \Omega_\Lambda\right]. \tag{C8}$$

Moreover, we assume that $\Omega_{\rm rad} \ll \Omega_{\rm dm}$, $\Omega_{\rm dm} \simeq 0.3$, and $\Omega_\Lambda \simeq 0.7$. Then, we can safely ignore Ω_Λ at the matter–radiation equality $\eta = \eta_{\rm eq}$, when $\rho_{\rm rad} = \rho_{\rm dm}$. This immediately implies

$$\frac{\Omega_{\rm rad}}{\Omega_{\rm dm}} = \frac{a(\eta_{\rm eq})}{a_0}.$$

Therefore, Equation (C8) implies

$$\mathcal{H}(\eta_{\rm eq}) = \frac{\mathcal{H}_0}{(a(\eta_{\rm eq})/a_0)^{1/2}}\sqrt{2\Omega_{\rm dm}}.$$

This corrects Equation (C2) or Equation (5.4) in De Luca et al. (2019). This gives a factor $\sqrt{2\Omega_{\rm dm}}$ on the rightmost side of Equations (C3) and (C4) and a factor $(2\Omega_{\rm dm})^{1/4}$ on the rightmost side of Equation (C5). Thus, there appears a factor $(2\Omega_{\rm dm})^{-1}$ on the rightmost side of Equation (C6), and this $\Omega_{\rm dm}^{-1}$ cancels out the factor $\Omega_{\rm dm}$ from ρ_b. Then, we reach the same expression as in Equation (C7).

ORCID iDs

Tomohiro Harada https://orcid.org/0000-0002-9085-9905

References

Abbott, B. P., LIGO Scientific & Virgo, et al. 2019, ApJL, 882, L24
Abbott, R., LIGO Scientific & Virgo, et al. 2020, PhRvD, 102, 043015
Arbey, A., Auffinger, J., & Silk, J. 2020, MNRAS, 494, 1257
Bardeen, J. M., Bond, J. R., Kaiser, N., & Szalay, A. S. 1986, ApJ, 304, 15
Bird, S., Cholis, I., Muñoz, J. B., et al. 2016, PhRvL, 116, 201301
Carr, B. J. 1975, ApJ, 201, 1
Carr, B. J., Kohri, K., Sendouda, Y., & Yokoyama, J. 2010, PhRvD, 81, 104019
Carr, B. J., Kohri, K., Sendouda, Y., & Yokoyama, J. 2020, arXiv:2002.12778
Carr, B. J., & Kühnel, F. 2019, PhRvD, 99, 103535
Carr, B. J., Kühnel, F., & Sandstad, M. 2016, PhRvD, 94, 083504
Carr, B. J., Raidal, M., Tenkanen, T., Vaskonen, V., & Veermäe, H. 2017, PhRvD, 96, 023514
Chiba, T., & Yokoyama, S. 2017, PTEP, 2017, 083E01
Clesse, S., & García-Bellido, J. 2017, PDU, 15, 142
Dasgupta, B., Laha, R., & Ray, A. 2020, PhRvL, 125, 101101
De Luca, V., Desjacques, V., Franciolini, G., Malhotra, A., & Riotto, A. 2019, JCAP, 05, 018
De Luca, V., Franciolini, G., Pani, P., & Riotto, A. 2020, JCAP, 04, 052
Escrivà, A. 2020, PDU, 27, 100466
Escrivà, A., Germani, C., & Sheth, R. K. 2020, PhRvD, 101, 044022
Germani, C., & Musco, I. 2019, PhRvL, 122, 141302
Harada, T., Yoo, C. M., & Kohri, K. 2013, PhRvD, 88, 084051
Harada, T., Yoo, C. M., Kohri, K., & Nakao, K. I. 2017, PhRvD, 96, 083517
Harada, T., Yoo, C. M., Nakama, T., & Koga, Y. 2015, PhRvD, 91, 084057
He, M., & Suyama, T. 2019, PhRvD, 100, 063520
Heavens, A., & Peacock, J. 1988, MNRAS, 232, 339
Kodama, H., & Sasaki, M. 1984, PThPS, 78, 1
Mirbabayi, M., Gruzinov, A., & Noreña, J. 2020, JCAP, 03, 017
Musco, I. 2019, PhRvD, 100, 123524
Musco, I., & Miller, J. C. 2013, CQGra, 30, 145009
Musco, I., Miller, J. C., & Polnarev, A. G. 2009, CQGra, 26, 235001
Nakamura, T., Sasaki, M., Tanaka, T., & Thorne, K. S. 1997, ApJL, 487, L139
Niemeyer, J. C., & Jedamzik, K. 1999, PhRvD, 59, 124013
Page, D. N. 1976, PhRvD, 14, 3260
Polnarev, A. G., & Musco, I. 2007, CQGra, 24, 1405
Raidal, M., Vaskonen, V., & Veermäe, H. 2017, JCAP, 09, 037
Sasaki, M., Suyama, T., Tanaka, T., & Yokoyama, S. 2016, PhRvL, 117, 061101
Shibata, M., & Sasaki, M. 1999, PhRvD, 60, 084002
Tokeshi, K., Inomata, K., & Yokoyama, J. 2020, JCAP, 12, 038
Wald, R. M. 1984, General Relativity (Chicago: Chicago Univ. Press) doi:10.7208/chicago/9780226870373.001.0001
Yoo, C. M., Harada, T., Garriga, J., & Kohri, K. 2018, PTEP, 2018, 123E01
Yoo, C. M., Harada, T., Hirano, S., & Kohri, K. 2021, PTEP, 2021, 013E02
Young, S. 2019, IJMPD, 29, 2030002